Electronic Supplementary Information for
Structure-Composition Trends in Multicomponent Borosilicate-Based Glasses Deduced from Molecular Dynamics Simulations with Improved B–O and P–O Force Fields

Baltzar Stevensson, Yang Yu, and Mattias Edén[*]

Physical Chemistry Division, Department of Materials and Environmental Chemistry, Stockholm University, SE-106 91 Stockholm, Sweden

[*]Corresponding author. E-mail: *mattias.eden@mmk.su.se*

Contents

S1 Force Field Validations on Crystalline Structures

The P–O and B–O force fields were evaluated by NPT energy minimizations at 0 K in vacuum by utilizing the GULP program[S1] to a set of P and/or B based crystalline structures, with the interatomic potentials evaluated out to 0.8 nm. The space-group symmetry was preserved throughout. Table **S2** contrasts the resulting lattice parameters $\{a, b, c\}$, and unit cell volume (V) with their experimental counterparts obtained by X-ray diffraction (XRD). An acceptable agreement is observed, with the calculated volumes generally staying within 95% and 92% of the experimental counterparts for the phosphates and borates, respectively, whereas similar errors resulted for the $\{a, b, c\}$ parameters. The B_2O_3 calculation manifests the overall largest deviation of $\approx$11% in the cell volume and 3–4% of the lattice parameters.

We are not aware of similar evaluations of B–O force fields on crystalline structures and the present results may therefore be viewed as benchmark values for future comparisons. Yet, we note that our P–O potential assessments on crystalline phosphates provide comparable deviations as those obtained by the shell-model-based P–O force field recently introduced by Ainsworth et al.,[S2] which was developed specifically for MD simulations of Na/Ca-bearing phosphate glasses. Further validations are discussed in the main article in the context of the B/P-bearing multicomponent glasses listed in Table **1**.

Table S1: MD Simulation Parameters[a]

Glass	Oxide Equivalents (mol%)					Number of Atoms							$N_{\rm sim}$	a (nm)[b]	ρ (g cm^{-3})[c]	Ref.
	Na_2O	CaO	B_2O_3	SiO_2	P_2O_5	$N_{\rm tot}$	$N_{\rm Na}$	$N_{\rm Ca}$	$N_{\rm B}$	$N_{\rm Si}$	$N_{\rm P}$	$N_{\rm O}$				
NB0.11	10.0		90.0			3504	146		1314			2044	3	3.446	2.040	S3
NB0.20	17.0		83.0			3495	255		1245			1995	3	3.413	2.140	S3
NB0.25	20.0		80.0			3519	306		1224			1989	3	3.394	2.213	S4
NB0.50	33.3		66.7			3510	540		1080			1890	3	3.364	2.370	S3
NB0.67	40.0		60.0			3507	668		1002			1837	3	3.385	2.380	S3
NB1.00	50.0		50.0			3500	875		875			1750	3	3.431	2.367	S3
NB1.30	56.5		43.5			3560	1040		800			1720	4	3.469	2.390	S3[d]
NBS2-0.25(33)	7.7		30.8	61.5		3478	148		592	592		2146	3	3.600	2.192	S5
NBS2-0.5(33)	14.3		28.6	57.1		6000	480		960	960		3600	3	4.188	2.396	S6
NBS2-0.75(33)	20.0		26.7	53.3		3498	396		528	528		2046	3	3.460	2.501	S7[d]
NBS2-2.5(33)	45.4		18.2	36.4		3515	950		380	380		1805	3	3.517	2.499	S7[d]
NBS0.5-0.5(67)	25.0		50.0	25.0		3504	438		876	219		1971	3	3.401	2.416	S8
NBS5.10-1.31(16)	17.7		13.5	68.8		3270	354		270	688		1958	4	3.446	2.503	S9
NBS4-4(20)	44.5		11.0	44.5		3509	968		242	484		1815	4	3.548	2.510	S7[d]
NCBPS(0)	24.1	23.3		48.6	4.0	5855	966	465		972	160	3292	3	4.287	2.650	S10
NCBPS(10)	24.1	23.3	4.9	43.7	4.0	6049	966	465	194	875	160	3389	2	4.298	2.649	S11
NCBPS(20)	24.1	23.3	9.7	38.9	4.0	6243	966	465	388	778	160	3486	2	4.308	2.648	S11
NCBPS(30)	24.1	23.3	14.6	34.0	4.0	6439	966	465	584	680	160	3584	2	4.321	2.645	S11
NCBPS(50)	24.1	23.3	24.3	24.3	4.0	6827	966	465	972	486	160	3778	2	4.357	2.616	S11
NCBPS(80)	24.1	23.3	38.9	9.7	4.0	7411	966	465	1556	194	160	4070	2	4.415	2.570	S11
NCPS[2.11]	24.6	26.7		46.1	2.6	5674	984	534		922	104	3130	2	4.230	2.704	S10
NCPS[2.30]	24.2	26.4		45.4	4.0	5792	968	528		908	160	3228	4	4.256	2.704	S10
NCPS[2.54]	24.1	23.3		48.6	4.0	5855	966	465		972	160	3292	3	4.287	2.650	S10
NCPS[2.74]	20.2	22.2		55.0	2.6	5887	824	454		1124	106	3379	4	4.296	2.640	S10
NCPS[2.93]	17.9	23.3		54.8	4.0	6372	776	508		1192	176	3720	2	4.414	2.639	S10

[a]$N_{\rm tot}$ represents the total number of atoms in the simulation of one glass model, with $\{N_{\rm Na}, N_{\rm Ca}, N_{\rm B}, N_{\rm Si}, N_{\rm P}, N_{\rm O}\}$ corresponding to those of {Na, Ca, B, Si, P, O}, respectively, while $N_{\rm sim}$ is the number of independent glass models generated.

[b]Side length of the cubic box.

[c]Experimental density, obtained from the as-indicated source.

[d]The experimental density is not available for the precise glass composition: ρ was estimated by interpolating between values reported for neighboring compositions.

Table S2: Optimized Cell Parameters of P/B-Bearing Structures[a]

	Space group	V (nm^3)[b]	$a/b/c$ (pm)[c]	$\epsilon_a/\epsilon_b/\epsilon_c$ (%)[d]	Ref.
Phosphates					
Na$_3$PO$_4$	$P\bar{4}2_1c$				
exp		0.7969	1081.1/1081.1/ 681.8		S12[e]
calc		0.7793(−2.2%)	1075.8/1075.8/ 673.4	−0.5/−0.5/−1.2	
NaCaPO$_4$	$Pna2_1$				
exp		1.0113	2039.7/ 916.1/ 541.2		S13
calc		1.0620(+5.0%)	2179.8/ 927.1/ 525.5	+6.9/+1.2/−2.9	
Na$_2$CaP$_2$O$_7$	$P\bar{1}$				
exp		0.3083	536.1/ 702.9/ 874.3		S14
calc[f]		0.3142(+1.9%)	543.2/ 704.2/ 871.0	+1.3/+0.2/−0.4	
SiP$_2$O$_7$	$P6_3$				
exp		0.2295	471.6/ 471.6/1191.7		S15[g]
calc		0.2321(+1.1%)	478.9/ 478.9/1168.6	+1.5/+1.5/−1.9	
Borates/Borosilicates					
B$_2$O$_3$	$P3_1$				
exp		0.1358	433.6/ 433.6/ 834.0		S16
calc		0.1211(−10.8%)	416.3/ 416.3/ 806.8	−4.0/−4.0/−3.3	
NaBO$_2$	$R\bar{3}c$				
exp		0.7930	1192.5/1192.5/ 643.9		S17
calc		0.7620(−3.9%)	1182.3/1182.3/ 629.5	−0.9/−0.9/−2.2	
CaB$_2$O$_4$	$Pbcn$				
exp		0.3073	620.5/1158.7/ 427.5		S18
calc		0.3119(+1.5%)	624.2/1211.5/ 412.5	+0.6/+4.6/−3.5	
Ca$_3$B$_2$O$_6$	$R\bar{3}c$				
exp		0.7648	863.1/ 863.1/1185.5		S19
calc		0.8248(+7.8%)	869.7/ 869.7/1259.0	+0.8/+0.8/+6.2	
Na$_3$CaB$_5$O$_{10}$	$P\bar{1}$				
exp		0.4404	746.0/ 744.5/1112.4		S20
calc[h]		0.4403(+0.0%)	752.8/ 738.5/1083.5	+0.9/−0.8/−2.6	
NaBSiO$_4$	$P6_3$				
exp		0.4307	803.5/ 803.5/ 770.3		S21
calc		0.4059(−5.8%)	788.6/ 788.6/ 753.5	−1.9/−1.9/−2.2	
CaB$_2$Si$_2$O$_8$	$Pnma$				
exp		0.5438	803.8/ 875.2/ 773.0		S22
calc		0.5345(−1.7%)	800.9/ 864.1/ 772.4	−0.4/−1.3/−0.1	
Borophosphates					
Na$_3$BP$_2$O$_8$	$C2/c$				
exp		1.3191	1256.7/1029.0/1021.0		S23
calc[i]		1.2596(−4.5%)	1209.8/1016.8/1024.0	−3.7/−1.2/+0.3	
CaBPO$_5$	$P3_121$				
exp		0.2555	668.0/ 668.0/ 661.2		S24[g]
calc		0.2512(−1.7%)	659.4/ 659.4/ 667.2	−1.3/−1.3/+0.9	

[a]Energy minimized lattice parameters obtained by the interatomic potential parameters listed in Table **2**. Experimental reference parameters were obtained by single-crystal XRD, unless noted otherwise.

[b]Cell volume, with values within parentheses representing relative deviations (in %) from the experimental value.

[c]$\{a, b, c\}$ unit cell parameters

[d]Relative deviations of the calculated $\{a, b, c\}$ parameters (listed in the previous column) relative to the experimental data.

[e]Data obtained from neutron powder diffraction.

[f]The relative error of the unit-cell angles $\{\alpha, \beta, \gamma\}$ are $\{1.8\%, 0.6\%, 0.1\%\}$.

[g]Data obtained by powder XRD.

[h]The $\{\alpha, \beta, \gamma\}$ angles were also optimized, giving relative errors of $\{0.8\%, 2.9\%, -2.7\%\}$.

[i]The angle β was optimized, yielding a relative error of -1.95%.

Table S3: Average F–O–F' Bond Angles[a]

Glass	x_{NBO}	$x_{\mathrm{B}}^{[4]}$	Si–O–Si	Si–O–B[3]	Si–O–B[4]	B[3]–O–B[3]	B[3]–O–B[4]	B[4]–O–B[4]
NB0.11	0.000	0.118				127.1	126.1	127.4
NB0.20	0.000	0.214				127.1	126.7	128.1
NB0.25	0.007	0.331				127.1	127.0	129.2
NB0.50	0.050	0.420				126.3	126.7	128.4
NB0.67	0.139	0.420				126.1	126.0	128.1
NB1.00	0.337	0.331				125.5	125.9	127.1
NB1.30	0.495	0.238				125.7	126.8	127.5
NBS2–0.25(33)	0.005	0.240	147.0	135.7	132.1	126.4	127.1	130.0
NBS2–0.50(33)	0.020	0.433	144.8	134.8	132.2	126.3	128.1	131.5
NBS2–0.75(33)	0.050	0.563	143.0	133.6	132.3	127.3	126.9	132.2
NBS2–2.50(33)	0.445	0.385	140.6	131.6	131.9	123.7	129.4	135.9
NBS0.5–0.50(67)	0.033	0.435	145.4	133.8	132.8	126.5	127.4	130.9
NBS5.10–1.31(16)	0.097	0.615	142.4	132.5	131.4	127.8	127.7	131.6
NBS4–4.00(20)	0.484	0.367	140.4	130.9	132.3	125.0	128.6	133.2
NCBPS(0)	0.625		138.5					
NCBPS(10)	0.584	0.403	138.5	129.8	130.0	124.2	126.7	138.4
NCBPS(20)	0.546	0.392	139.2	130.4	130.0	124.0	127.6	133.3
NCBPS(30)	0.504	0.431	139.8	129.8	130.6	126.8	127.1	129.7
NCBPS(50)	0.438	0.420	140.1	130.6	130.3	124.5	126.1	130.0
NCBPS(80)	0.348	0.419	141.5	132.2	130.5	125.8	125.8	128.7
NCPS[2.11]	0.688		137.0					
NCPS[2.30]	0.677		137.4					
NCPS[2.54]	0.625		138.5					
NCPS[2.74]	0.544		138.8					
NCPS[2.93]	0.529		139.4					
$\sigma^{\mathbf{b}}$	0.001	0.007	0.3	0.4	0.3	1.1	0.7	2.0

[a]Corner-shared average interpolyhedral angles in degrees.

[b]Typical data uncertainties, estimated as the rms deviation from the average parameter value.

**Table S4: Distribution of Na$^{[p]}$ and Ca$^{[p]}$ Coordinations[a]**

Glass	x_{NBO}	$x_{\text{B}}^{[4]}$	$\overline{Z}_{\text{Na}}$	$\sigma_{\text{Na}}(p)$	$x_{\text{Na}}^{[4]}$	$x_{\text{Na}}^{[5]}$	$x_{\text{Na}}^{[6]}$	$x_{\text{Na}}^{[7]}$	$x_{\text{Na}}^{[8]}$	$x_{\text{Na}}^{[9]}$	$\overline{Z}_{\text{Ca}}$	$\sigma_{\text{Ca}}(p)$	$x_{\text{Ca}}^{[4]}$	$x_{\text{Ca}}^{[5]}$	$x_{\text{Ca}}^{[6]}$	$x_{\text{Ca}}^{[7]}$	$x_{\text{Ca}}^{[8]}$	$x_{\text{Ca}}^{[9]}$
NB0.11	0.000	0.118	7.30	1.11	0.003	0.039	0.186	0.355	0.282	0.111								
NB0.20	0.000	0.214	7.23	1.13	0.004	0.050	0.200	0.346	0.274	0.107								
NB0.25	0.007	0.331	6.99	1.24	0.015	0.094	0.235	0.322	0.229	0.084								
NB0.50	0.050	0.420	6.91	1.30	0.024	0.108	0.247	0.298	0.213	0.087								
NB0.67	0.139	0.420	6.56	1.29	0.043	0.155	0.291	0.282	0.157	0.056								
NB1.00	0.337	0.331	6.14	1.17	0.063	0.234	0.337	0.242	0.094	0.021								
NB1.30	0.495	0.238	6.00	1.07	0.056	0.280	0.368	0.213	0.068	0.013								
NBS2–0.25(33)	0.005	0.240	6.21	1.28	0.073	0.207	0.317	0.246	0.107	0.034								
NBS2–0.50(33)	0.020	0.433	6.42	1.26	0.048	0.179	0.296	0.279	0.142	0.043								
NBS2–0.75(33)	0.050	0.563	6.54	1.31	0.047	0.163	0.280	0.282	0.160	0.052								
NBS2–2.50(33)	0.445	0.385	5.78	1.06	0.095	0.314	0.354	0.178	0.047	0.007								
NBS0.5–0.50(67)	0.033	0.435	6.83	1.27	0.021	0.118	0.270	0.307	0.190	0.074								
NBS5.10–1.31(16)	0.097	0.615	6.04	1.27	0.092	0.229	0.318	0.221	0.097	0.025								
NBS4–4.00(20)	0.484	0.367	5.63	1.00	0.113	0.349	0.355	0.143	0.032	0.003								
NCBPS(0)	0.625		5.84	1.00	0.071	0.299	0.388	0.191	0.043	0.004	5.91	0.83	0.031	0.270	0.482	0.190	0.025	0.001
NCBPS(10)	0.584	0.403	5.95	1.01	0.062	0.261	0.391	0.223	0.053	0.005	6.03	0.84	0.014	0.252	0.470	0.222	0.040	0.002
NCBPS(20)	0.546	0.392	6.09	1.03	0.045	0.241	0.386	0.242	0.074	0.011	6.16	0.90	0.016	0.208	0.445	0.261	0.064	0.005
NCBPS(30)	0.504	0.431	6.24	1.09	0.043	0.203	0.366	0.266	0.100	0.019	6.19	0.92	0.016	0.206	0.436	0.269	0.065	0.009
NCBPS(50)	0.438	0.420	6.37	1.13	0.037	0.184	0.336	0.291	0.120	0.028	6.43	1.00	0.012	0.148	0.397	0.306	0.111	0.023
NCBPS(80)	0.348	0.419	6.61	1.23	0.028	0.152	0.304	0.293	0.157	0.054	6.64	1.07	0.008	0.122	0.345	0.323	0.157	0.039
NCPS[2.11]	0.688		5.87	0.94	0.054	0.293	0.419	0.190	0.037	0.004	5.96	0.82	0.023	0.256	0.494	0.199	0.027	0.001
NCPS[2.30]	0.677		5.94	0.96	0.050	0.273	0.406	0.220	0.045	0.003	6.00	0.83	0.018	0.245	0.482	0.219	0.034	0.002
NCPS[2.54]	0.625		5.84	1.00	0.071	0.299	0.388	0.191	0.043	0.004	5.91	0.83	0.031	0.270	0.482	0.190	0.025	0.001
NCPS[2.74]	0.544		5.82	1.02	0.079	0.298	0.381	0.187	0.046	0.004	5.85	0.85	0.035	0.306	0.462	0.166	0.028	0.002
NCPS[2.93]	0.529		5.89	1.05	0.077	0.274	0.377	0.204	0.056	0.006	5.94	0.89	0.034	0.274	0.450	0.204	0.034	0.004
σ[b]	0.001	0.007	0.02	0.02	0.004	0.005	0.008	0.006	0.003	0.003	0.02	0.01	0.003	0.008	0.009	0.006	0.006	0.001

[a]Fractional populations $\{x_M^{[p]}\}$ of $\{M^{[p]}\}$ coordinations for $M=\{$Na,Ca$\}$, average coordination number $\overline{Z}_M = \sum_p p x_M^{[p]}$, and distribution width $\sigma_M(p) = \left\{\sum_p x_M^{[p]}(p - \overline{Z}_M)^2\right\}^{1/2}$. The fractional populations obey $\sum_p x_M^{[p]} = 1$, but a few structures involve minor $M^{[3]}$ or $M^{[10]}$ contributions (not listed).

[b]Typical data uncertainties, estimated as the rms deviation from the average parameter value.
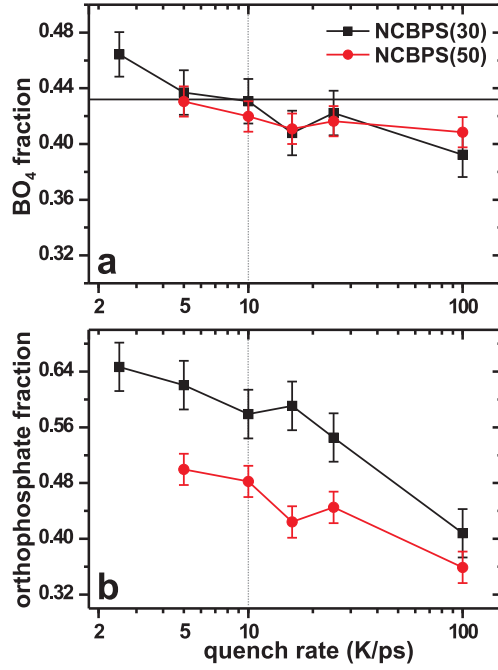
Fig. S1. Cooling-rate (q) dependence of the MD-generated fractional population of (a) BO_4 and (b) orthophosphate groups in the NCBPS(30) and NCBPS(50) glasses. The vertical line marks the rate $q = 10$ K/ps employed in all other simulations. Both glasses reveal very close NMR-derived values $x_B^{[4]} \approx 0.43$ in (a), marked by the horizontal line. Note that the two NMR-derived orthophosphate fractions, $x_P^0 = 0.89$ for NCBPS(30) and $x_P^0 = 0.86$ for NCBPS(50), are outside the vertical plot-range in (b).
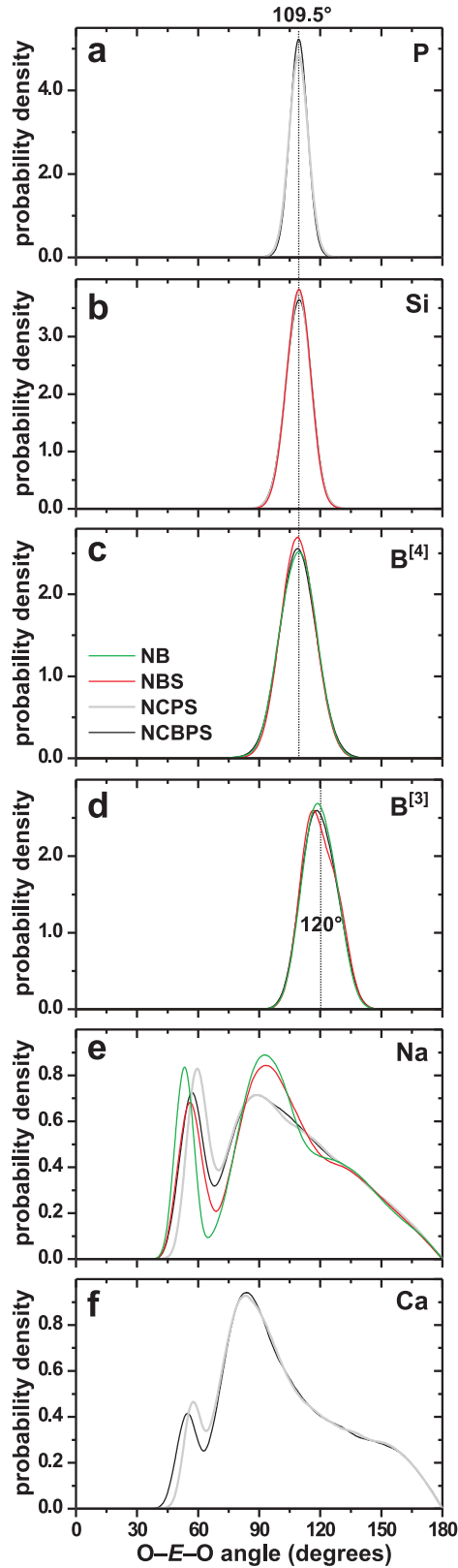
Fig. S2. Intrapolyhedral O–*E*–O bond-angle distribution (BAD) functions observed in models of the NB1.3, NBS2–2.5(33), NCPS[2.93], and NCBPS(30) glasses [see legend in (c)] for the network formers (a) P, (b) Si, (c) B[4], (d) B[3], as well as the network modifiers (e) Na, and (f) Ca. The glasses feature $x_{\mathrm{NBO}} \approx 0.5$ (see caption to Fig. **5** for further details).
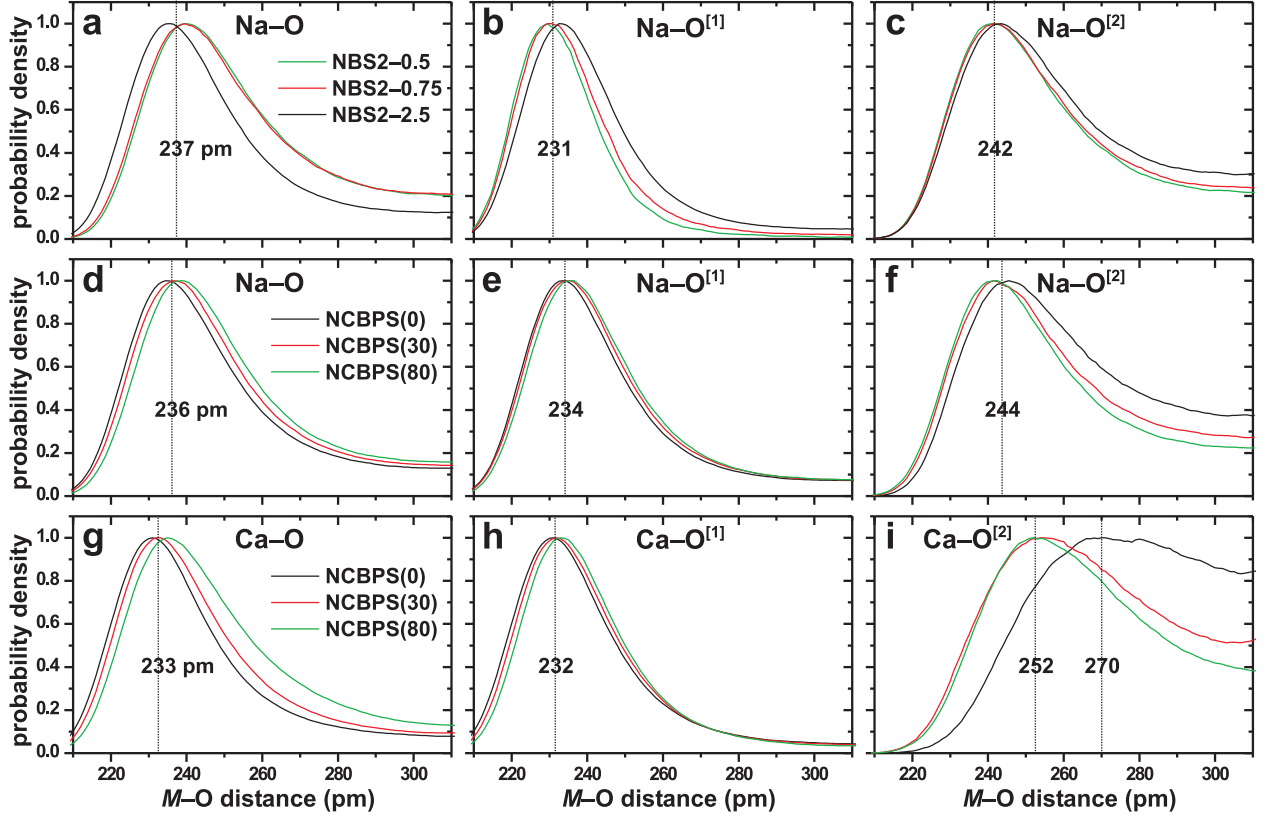
Fig. S3. MD-derived M–O (left panel), M–O[1] (mid panel), and M–O[2] (right panel) pair-distribution functions for (a–f) M=Na, and (g–i) M=Ca in glass models of the (a–c) NBS and (d–g) NCBPS systems, as identified by the legends in (a, d, g). Note that the NBO content *increases* together with R along the NBS2–R(33) series, whereas it *decreases* for increasing amount of B in the NCBPS(f) glasses (i.e., for increasing f). To facilitate comparisons among different O[1]/O[2] coordinations and glasses with distinct NBO contents, all PDFs are normalized to equal maxima of unity.

References

S1 J. D. Gale and A. L. Rohl, *Mol. Simul.*, 2003, **29**, 291–341.

S2 R. I. Ainsworth, D. Di Tommaso, J. K. Christie, and N. H. de Leeuw, *J. Chem. Phys.*, 2012, **137**, 234502.

S3 D. Fail and S. Feller, *J. Non-Cryst. Solids*, 1990, **119**, 103–111.

S4 J. D. Epping, H. Eckert, A. W. Imre, and H. Mehrer, *J. Non-Cryst. Solids*, 2005, **351**, 3521–3529.

S5 K. Takahashi, A. Osaka, and R. Furuno, *Yogyo Kyokai Shi*, 1983, **91**, 199–205.

S6 M. Ren, L. Deng, and J. Du, *J. Am. Ceram. Soc.*, 2017, **100**, 2516–2524.

S7 M. Barlet, A. Kerrache, J.-M. Delaye, and C. L. Rountree, *J. Non-Cryst. Solids*, 2013, **382**, 32–44.

S8 M. Imaoka, H. Hasegawa, Y. Hamaguchi, and Y. Kurotaki, *Yogyo Kyokai Shi*, 1971, **79**, 36–44.

S9 W. L. Konijnendijk, *The Structure of Borosilicate Glasses*, Technische Hogeschool Eindhoven, Eindhoven, 1975.

S10 R. Mathew, B. Stevensson, A. Tilocca, and M. Edén, *J. Phys. Chem. B*, 2014, **118**, 833–844.

S11 Y. Yu, B. Stevensson, and M. Edén, *J. Phys. Chem. B*, 2017, **121**, 9737–9752.

S12 R. J. Harrison, A. Putnis, and W. Kockelmann, *Phys. Chem. Chem. Phys.*, 2002, **4**, 3252–3259.

S13 M. Ben Amara, M. Vlasse, G. Le Flem, and P. Hagenmuller, *Acta Cryst.*, 1983, **C39**, 1483–1485.

S14 J. Bennazha, A. Boukhari, and E. M. Holt, *Solid State Sci.*, 1999, **1**, 373–380.

S15 D. M. Poojary, R. B. Borade, F. L. Cambell III, and A. Clearfield, *J. Solid State Chem.*, 1994, **112**, 106–112.

S16 G. E. Gurr, P. W. Montgomery, C. D. Knutson, and B. T. Gorres, *Acta Cryst.*, 1970, **B26**, 906–915.

S17 M. Marezio, H. A. Plettinger, and W. H. Zachariasen, *Acta Cryst.*, 1963, **16**, 594–595.

S18 A. Kirfel, *Acta Cryst.*, 1987, **B43**, 333–343.

S19 W. Schuckmann, *Neues Jahrb. Mineral. Mh.*, 1969, **1969**, 142–143.

S20 J. Fayos, R. A. Howie, and F. P. Glasser, *Acta Cryst.*, 1985, **C41**, 1396–1398.

S21 E. V. Sokolova and A. P. Khomyakov, *Dokl. Akad. Nauk SSSR*, 1991, **319**, 879–883.

S22 M. W. Phillips, G. V. Gibbs, and P. H. Ribbe, *Am. Mineral.*, 1974, **59**, 79–85.

S23 D.-B. Xiong, H.-H. Chen, X.-X. Yang, and J.-T. Zhao, *J. Solid State Chem.*, 2007, **180**, 233–239.

S24 R. Kniep, G. Gözel, B. Eisenmann, C. Röhr, M. Asbrand, and M. Kizilyalli, *Angew. Chem. Int. Ed.*, 1994, **33**, 749–751.